



Swansea University
Prifysgol Abertawe



Cronfa - Swansea University Open Access Repository

This is an author produced version of a paper published in:
Annals of Neurology

Cronfa URL for this paper:
<http://cronfa.swan.ac.uk/Record/cronfa39104>

Paper:

Magliozzi, R., Howell, O., Nicholas, R., Cruciani, C., Castellaro, M., Romualdi, C., Rossi, S., Pitteri, M., Benedetti, M., et. al. (in press). Inflammatory intrathecal profiles and cortical damage in multiple sclerosis. *Annals of Neurology*
<http://dx.doi.org/10.1002/ana.25197>


This item is brought to you by Swansea University. Any person downloading material is agreeing to abide by the terms of the repository licence. Copies of full text items may be used or reproduced in any format or medium, without prior permission for personal research or study, educational or non-commercial purposes only. The copyright for any work remains with the original author unless otherwise specified. The full-text must not be sold in any format or medium without the formal permission of the copyright holder.

Permission for multiple reproductions should be obtained from the original author.

Authors are personally responsible for adhering to copyright and publisher restrictions when uploading content to the repository.

<http://www.swansea.ac.uk/library/researchsupport/ris-support/>

Inflammatory intrathecal profiles and cortical damage in multiple sclerosis

*R. Magliozzi^{1,2}, *O.W. Howell³, R. Nicholas², C. Cruciani^{1,2}, M. Castellaro⁴, C. Romualdi⁵, S. Rossi^{1,6}, M. Pitteri¹ , M.D. Benedetti¹, A. Gajofatto¹, F.B. Pizzini⁷, S. Montemezzi⁷, S. Rasia⁸, R. Capra⁸, A. Bertoldo⁵, F. Facchiano⁶, S. Monaco¹, [§]R. Reynolds² and [§]M. Calabrese¹

Institution(s):

¹Neurology B, Dept. of Neurological and Movement Sciences, University of Verona, Italy

²Division of Brain Sciences, Department of Medicine, Imperial College London, United Kingdom,

³Institute of Life Sciences, Swansea University, Swansea, United Kingdom

⁴Department of Information Engineering, University of Padova, Padova, Italy

⁵ Department of Biology, University of Padova, Padova, Italy

⁶Istituto Superiore di Sanità, Department of Oncology and Molecular Medicine, Rome, Italy

⁷Neuroradiology & Radiology Units, Department of Diagnostic and Pathology, University Hospital of Verona, Verona, Italy

⁸Multiple Sclerosis Center, ASST Spedali Civili, P.O. Montichiari, Brescia, Italy

* these authors equally contributed to the manuscript.

[§] Joint corresponding authors:

Prof. Massimiliano Calabrese

Neurology B, Department of Neurosciences, Biomedicine and Movement Sciences

University of Verona, Italy

Address: Policlinico "G.B. Rossi" Borgo Roma

Piazzale L. A. Scuro, 10, 37134 Verona, Italy

Phone (shared): +39.045.8124.678

Fax (shared): +39.045.8027.492

E-mail: massimiliano.calabrese@univr.it

Prof. Richard Reynolds,

Division of Brain Sciences,

Faculty of Medicine, Imperial College London,

This article has been accepted for publication and undergone full peer review but has not been through the copyediting, typesetting, pagination and proofreading process which may lead to differences between this version and the Version of Record. Please cite this article as an 'Accepted Article', doi: 10.1002/ana.25197

This article is protected by copyright. All rights reserved.

Hammersmith Hospital Campus,
Imperial College London,
London W12 0NN.

Phone: +44 0207 594 6668

E-mail: r.reynolds@imperial.ac.uk

Running title: Intrathecal inflammation and cortical pathology in MS

Accepted Article

Abstract

Objective: Grey matter (GM) damage and meningeal inflammation have been associated with early disease onset and a more aggressive disease course in Multiple Sclerosis (MS), but can these changes be identified in the patient early in the disease course?

Methods: To identify possible biomarkers linking meningeal inflammation, GM damage and disease severity, gene and protein expression were analysed in meninges and CSF from 27 post-mortem secondary progressive MS (SPMS) and 14 control cases. Combined cytokine/chemokine CSF profiling and 3T-MRI were performed at diagnosis in two independent cohorts of MS patients (35 and 38 subjects) and in 26 non-MS patients.

Results: Increased expression of pro-inflammatory cytokines (IFN γ , TNF, IL2 and IL22) and molecules related to sustained B-cell activity and lymphoid-neogenesis (CXCL13, CXCL10, LT α , IL6, IL10) was detected in the meninges and CSF of post-mortem MS cases with high levels of meningeal inflammation and GM demyelination. Similar pro-inflammatory patterns, including increased levels of CXCL13, TNF, IFN γ , CXCL12, IL6, IL8 and IL10, together with high levels of BAFF, APRIL, LIGHT, TWEAK, sTNFR1, sCD163, MMP2 and pentraxin III, were detected in the CSF of MS patients with higher levels of GM damage at diagnosis.

Interpretation: A common pattern of intrathecal (meninges and CSF) inflammatory profile strongly correlates with increased cortical pathology, both at time of the diagnosis and of death. These results suggest a role for detailed CSF analysis combined with MRI, as a prognostic marker for more aggressive MS.

INTRODUCTION

Disability progression in MS patients is accompanied by the accumulation of chronic white matter (WM) demyelination with limited repair, axonal loss, diffuse inflammatory changes in the normal appearing WM^{1,2} and both focal and diffuse cortical grey matter (GM) demyelination and neurodegeneration³⁻⁶. Neuroimaging has confirmed that cortical lesions and GM atrophy are strongly related to physical disability⁷⁻⁹ and that these are present from the earliest stages of the disease^{4,10,11} suggested that leptomeningeal immune cell infiltration and compartmentalized inflammation within the subarachnoid space may play a key role in the pathogenesis of this cortical pathology^{5,11,15-17}. Increased meningeal inflammation is associated with a gradient of neuronal, astrocyte and oligodendrocyte damage and with microglial activation, which was higher in the superficial cortical layers (I-III)^{5,14}. A strong association between meningeal inflammation and the severity of underlying pathology is also seen in the spinal cord and cerebellum, in primary progressive MS and in the brain biopsies of patients with a recent diagnosis of MS^{11,18-20}.

Early in vivo detection of cortical pathology is vital in order to be able to effectively target the underlying mechanisms of progressive disease before significant disability develops. Cortical pathology could potentially be a biomarker indicating underlying compartmentalised inflammation. However, the in vivo detection of cortical lesions using MRI is still sub-optimal^{21,22} despite several improvements including the introduction of GM specific pulse sequences^{8,21,23-25} at high field 3T and ultra-high field 7T MRI^{26,27}. Therefore, there is a need for additional surrogate biomarkers of cortical GM demyelination and neurodegeneration and compartmentalised meningeal inflammation in order to identify early in the disease course those individuals at risk of a more severe disease course.

Several fluid biomarker studies have revealed the differential expression of individual CSF proteins in MS compared to controls. The presence of high levels of the neurofilament light-chain (NFL) protein is associated with a higher risk of conversion to clinically definite MS and/or increased brain and spinal cord atrophy²⁸. Increased levels of pro-inflammatory cytokines and chemokines, such as CXCL13²⁹, CXCL12²⁹, TNF^{30,31}, and IFN γ ³² are detected in the CSF of MS patients. However, an association between the presence of these or other inflammatory mediators in the CSF, and increased GM pathology and clinical outcomes has not yet been shown. Our previous studies using post-mortem analysis of paired CSF and meningeal samples, obtained from MS cases with or without meningeal lymphoid like tissues¹⁵, has suggested that increased TNF and IFN γ expression is associated with more severe cortical pathology.

Here we undertook a systematic and more comprehensive analysis of inflammatory and cytotoxic molecules expressed in the meninges and CSF derived from 27 post-mortem secondary

progressive MS (SPMS), stratified according to the level of meningeal inflammation and cortical demyelination, and 14 controls. This was then compared with the profile of inflammation related molecules in diagnostic CSFs in two independent cohorts of patients with MS, stratified by the presence of low or high numbers of cortical lesions determined by 3D-DIR MRI imaging, a training set (TS: 35 subjects) and a validation set (VS: 38 subjects), with the overall aim of determining whether cytokine profiles indicating greater cortical damage and a more rapidly progressive disease course could also be found in newly diagnosed MS patients.

METHODS

Study populations and subgroup classification

Post-mortem MS and control cohort

Snap frozen tissue blocks from 27 SPMS and 14 non-MS control (Ctrl) (without any evidence of neuropathology) post-mortem brains (Table 1) were obtained from the UK MS Society Tissue Bank at Imperial College (Ethical approval: National Research Ethics Committee: 08/MRE09/31). Three snap frozen cortical tissue blocks (2x2x1cm), representative of different regions of the frontal and temporal cortex, were examined from every SPMS case and were screened for the presence and extent of GM demyelination and the degree of meningeal inflammation^{6,14,33}. Fifteen SPMS cases were classified by a low level of meningeal inflammation and demyelination (PM-MSlow) and 12 by a high level of meningeal inflammation and demyelination (PM-MShigh), as previously described⁶. The degree of meningeal inflammation was assessed by manually counting the number of haematoxylin stained cell nuclei in 2 meningeal infiltrates for each examined tissue block (Fig 1A). The presence and extent of subpial (type III) GM demyelination was then assessed in all tissue blocks using immunohistochemistry for myelin oligodendrocyte glycoprotein (MOG) and the percentage of demyelinated GM with respect to the total GM calculated (Fig 1B) following the procedures previously optimized¹⁴. Not all MS and control cases from which the meningeal RNA had been prepared also had a paired CSF sample available. Therefore, for the CSF analysis, we included further samples from cases of SPMS for which the degree of inflammation and demyelination had been assessed in the same way (for details see Table 1).

MS patient cohorts

Seventy-eight consecutive treatment naïve relapsing remitting MS patients from the MS Centre of Verona University Hospital (Italy) were screened at diagnosis between September 2014 and February 2015. A first Training set (TS) cohort comprising 35 RRMS patients was enrolled. Inclusion criteria were the presence of at least 10 cortical lesions or less than 2 cortical lesions that permitted the stratification of the cohort into two subsets (TS-MShigh and TS-MSlow). Forty-three patients were excluded as that they did not meet the inclusion criteria.

A second independent group of 38 treatment naïve MS patients (Table 2) from the MS Centre of Verona University Hospital (29 patients) and the MS Centre of Montichiari (9 patients) were consecutively recruited (March 2015 to August 2015) at diagnosis without any bias with respect to the GM and WM lesion load and were termed the Validation Set (VS). They were age and sex matched with the TS group. Each patient was then assigned to a low (VS-MSlow) or high (VS-MShigh) group based on whether their cortical lesion count was above or below the median number of 7 cortical lesions for the whole cohort (Table 2 and Fig 3).

All the MS patients had a confirmed diagnosis of MS³⁴ and underwent neurological evaluation, 3T-MRI and CSF examination.

Twelve subjects with non-inflammatory neurological diseases (NIND), including 3 cerebrovascular diseases, 3 degenerative disease, 2 periphery neuropathies, 2 headache/dizziness without any CNS abnormality, 2 ischemic white matter lesions, and 14 subjects with other inflammatory neurological diseases (OIND), including 3 immune-mediated encephalitis, 2 neuromyelitis optica, 2 neurosarcoidosis, 2 leucoencephalopathies, 2 CNS paraneoplastic syndrome, 2 CNS vasculitis, 1 Behcet's disease, were also recruited at the time of the diagnosis. They also underwent neurological evaluation, 3T-MRI and CSF examination.

The local Ethic Committee approved the study. Informed consent was obtained from the patients.

Post-mortem study

Meningeal dissection and gene expression analysis

Meningeal tissues closely adjacent to the areas of either subpial cortical demyelination or normal appearing GM, were dissected from snap frozen tissue blocks from 20 SPMS and 10 controls (Table 1), as previously described^{5,15}. To obtain a sufficient amount of RNA for gene expression analysis the RNA obtained from 3 tissue blocks per case was pooled. RNA extractions were performed using the RNeasy Lipid Tissue Midi Kit (Qiagen), following procedures previously optimized for use with human tissues³⁵. The RNA concentration and quality were determined using a Nanodrop 2000 spectrophotometer and Agilent 2100 Bioanalyzer respectively.

Gene expression analysis of 84 human cytokines and chemokines was performed using a Qiagen RT Profile array (Human Cytokines & Chemokines RT2 Profiler PCR Array, cat. No. PAHS-150Z), following the manufacturer's instructions, including the pre-amplification step (12 cycles of 15s at 95C and 2 min at 60C). All samples were run in triplicate and the results analysed by two independent operators (R.M. and C.C.).

Post-mortem CSF protein analysis

The protein levels of 30 inflammatory cytokines and chemokines (V-PLEX Plus Human Cytokine 30-Plex kit) were determined in the post-mortem CSF obtained at autopsy from 20 SPMS (10 PM-MShigh and 10 PM-MSlow meningeal inflammation, Table 2) and 10 healthy controls using the MesoScale Discovery electrochemiluminescence system (MSD; Meso Scale Diagnostics, Rockville, MD; Supplementary Table 1). The MSD detection system was used with the manufacturer's protocol and provided a combination of high sensitivity with low background and a 5 log order of magnitude dynamic range.

Clinical study

Patient CSF protein analysis

CSF samples were obtained at least 2 months after the last relapse and within one week of the MRI, according to Consensus Guidelines for CSF and Blood Biobanking³⁶. After centrifugation, the supernatant and the cell pellet were stored separately at -80 °C until use. Immunoglobulin-G (Ig-G) index and presence/absence of oligoclonal bands (OCB) for each MS patient is reported in Table 2. The CSF analysis was optimized and performed by two independent investigators (R.M. and S.R.), blinded with respect to the clinical and MRI features. The levels of neurofilament protein light chain (NF-L) in CSF were measured using the Human NF-light ELISA kit (MyBioSource, San Diego, CA, USA) according to the manufacturer's instructions and the quantification was carried out on a VICTOR X3 2030 Multilabel Plate Reader (Perkin Elmer, Walluf, Germany). Intra-assay variability (coefficients of variation) of the samples was below 10%.

The levels of 69 inflammatory mediators (Supplementary Table 2) were assessed using a combination of immune-assay multiplex techniques based on the Luminex technology (40- and 37-Plex, Bio-Plex X200 System equipped with a magnetic workstation, BioRad, Hercules, CA, USA). All samples were run in duplicate in the same experiment and in two consecutive experiments, in order to verify the reproducibility and consistency of the results. The CSF level of each protein detected during the analysis was normalized to the total protein concentration of each CSF sample (measured by Bradford protocol). When comparing the two groups of 14 NIND and 12 OIND

controls, no differences were revealed in the presence and levels of the examined molecules. Therefore, the two groups were included as a single control group.

MRI Acquisition Protocol and analysis

Three tesla MRI was performed on each patient at least 2 months from the last relapse, at the Radiology unit of the University Hospital of Verona (Borgo Trento). MRI sequences were acquired using a Philips Achieva 3T MR Scanner. The following image sets were acquired:

- a) 3D T1 weighted Turbo Field Echo (TFE) (Repetition Time (TR) / Echo Time (TE)= 8.4/3.7ms, voxel size of 1x1x1 mm), Total acquisition time of 5:51 min;
- b) 3D Double Inversion Recovery (DIR) (TR/TE=5500/292ms, Inversion Times (TI) TI1/TI2=525ms/2530ms voxel size of 1x1x1mm), Turbo Spin Echo (TSE) read out with an optimal variable flip angle scheme, number of excitations 3, total acquisition time of 10:49 min; and
- c) 3D Fluid Attenuated Inversion Recovery (FLAIR) (TR/TE=5500/292ms, TI=1650ms voxel size of 1x1x1mm), same TSE readout as the DIR sequence, number of excitations 1, total acquisition time of 5:44 min.

MRI analysis

A. White matter lesion detection and lesion load assessment.

A semiautomatic lesion segmentation technique, included in MIPAV (Medical Image Processing and Visualization. <http://mipav.cit.nih.gov>) software, was applied to FLAIR images, to identify and segment WM lesions, thus obtaining a T2 hyperintense WM lesion volume (T2WMLV) at baseline.

B. Cortical lesion number and volume

The number of cortical lesions was assessed on DIR images following the recent recommendations for cortical lesions scoring in patients with MS³⁷. Such number included both intracortical and mixed (white matter/grey matter) lesions. In order of being as specific as possible, we have also calculated the number of intracortical lesions alone.

The total CL volume and the volume of intracortical lesions were calculated using a semiautomatic thresholding technique based on a Fuzzy C-mean algorithm³⁸ included in software developed at the National Institutes of Health, Medical Images Processing, Analysis and Visualization (<http://mipav.cit.nih.gov>).

C. Cortical thickness evaluation.

The estimation of the cortical thickness was performed using the 3D T1 TFE sequence and the automated, volume-based Advanced Normalization Tools (ANTs)³⁹ and, in particular, the ANTs Cortical Thickness pipeline³⁹. Particular attention was paid to exclude WM lesions that could hamper the estimation of atrophy even with a low WM lesion load³⁹. Therefore, the segmentation of T2 hyperintensity obtained in step A was used as a mask for the lesion filling of 3D T1. The co-registration of T1 and FLAIR images was operated with a rigid body transformation with ANTs. The mask was then moved onto the 3D T1. The lesion filling was operated with the lesion filling routine included in Lesion Segmentation Tool⁴⁰. The 3D T1 after lesion filling was then visually evaluated and manually corrected (the lesion filling step was run a second time with the new manually corrected lesion mask).

Statistical analysis

For the neuropathological and clinical study, differences among groups were assessed through analysis of variance (ANOVA). Age was used as a correction covariate and post hoc Tukey HSD procedure to account for multiple comparisons. Rank-based non-parametric tests (Kruskal-Wallis and Wilcoxon) were used when the data did not follow a normal distribution (Shapiro test). The Pearson Chi Square test was applied to test the difference between groups in terms of male/female ratio, patients with and without IgG oligoclonal bands and patients with polysymptomatic onset. False discovery rate (FDR) with significance level of 0.05 was adopted to correct for the multiple testing problem in the analysis of the CSF protein expression.

In order to evaluate the specificity and sensitivity of each molecule in predicting high or low cortical damage, different thresholds for each molecule were used to classify patients as MS_{low} or as MS_{high} and for each identified threshold the number of true positives and false positives were recorded in a ROC curve (Supplementary Table 3).

For the multivariate analysis, we utilised as independent variables those cytokines that were consistently raised across both post-mortem and in vivo groups and those that were raised in both patient groups and neurofilament protein light levels. Models were run using both cortical lesion number and cortical volume as an outcome using the total population.

RESULTS

Study cohorts and subgroup classification - post mortem cohort

Post-mortem SPMS cases were stratified according to the degree of meningeal inflammation: the PM-MS_{low} group (Table 1; Fig 1 A, C, E), with a low density of diffuse meningeal inflammation, and the PM-MS_{high} group, characterised by a significantly increased

degree of meningeal inflammatory infiltration (6.5 fold change, $p < 0.0001$; Fig 1A, D, F, G-I). In particular, a high frequency of immune cell aggregates rich in CD20+ B cells and CD3+ T cells (Fig 1G-I) was present in the subarachnoid space in the PM-MShigh group (Table 1; Fig 1 F-I). The PM-MShigh group was also characterized by a significant increase (2.9-fold, $p < 0.0001$) in the percentage of GM demyelination (Fig 1B; mean=70.03%; range= 56-82%) compared to the PM-MSlow group (Fig 1B; mean=28.7%; range=6-51%). In addition, the PM-MShigh group had a significantly earlier age at use of a wheelchair and at death (36.6 ± 7.39 , 47.1 ± 7.2) when compared to the PM-MSlow group (46 ± 6.43 , $p = 0.012$; 56.4 ± 6.13 , $p = 0.015$), but no significant difference in disease duration.

Increased meningeal inflammation in the post-mortem MS brain is associated with elevated gene expression of pro-inflammatory mediators

Significantly elevated gene expression for the pro-inflammatory molecules TNF, IFN γ , IL2, IL22, CXCL9, CXCL10, CXCL13, CXCL20 and CCL22 was found in the meninges of the PM-MShigh group compared to controls, whereas IL9, IL17 and IL22 (Fig 2A) gene expression was up-regulated in the PM-MSlow group compared to controls. A significant increase in the expression of the CXCL9, CXCL10, CXCL13 and TNF (Fig 2A) genes was found in the meninges of the PM-MShigh group compared to the PM-MSlow group, whereas IL17A (Fig 2A) gene expression was elevated in the PM-MSlow compared to the PM-MShigh group.

Significantly higher protein levels of TNF, LT α , IFN γ , CXCL10, CXCL13, CCL17, CCL22, IL2, IL10, IL12p40 and IL16 were found in the CSF of PM-MShigh compared to controls and only IL-4 was increased in the CSF of PM-MSlow compared to controls (Fig 2B). When the PM-MShigh cases were compared to the PM-MSlow cases, there was a significant increase in the levels of TNF, LT α , CXCL13, CCL22 and IL12p40 (Fig 2B). In contrast, only IL4 protein was increased in the CSF of PM-MSlow compared with the control group (Fig 2B). There was no significant difference in the CSF protein levels of IL17 between the groups (not shown).

Study populations and subgroup classification – in vivo patient population

The demographics and clinical features of the TS population are described in Table 2. Fifteen patients were classified as TS-MSlow and 20 patients as TS-MShigh on the basis of the number of total cortical lesions (see methods). Compared to the TS-MSlow group (Fig 3A), TS-MShigh patients (Fig 3B) were characterized by higher cortical lesion load (16.8 ± 6.4 vs 0.3 ± 0.5 , $p < 0.0001$) (Table 2), higher EDSS (2 vs 1.5, $p = 0.017$), higher T2WMLV (5.6 ± 1.6 vs 4.7 ± 1.6 ,

p=0.031) and lower mean cortical thickness over the entire brain (2.53 ± 0.34 vs 2.72 ± 0.41 , p=0.032) (Table 2).

When the number of merely intracortical lesions (including cortical lesion type II and III) was used to classify the patients such classification did not change: higher cortical lesion load was indeed found in T-MShigh compared to T-MSlow (7.55 ± 3.6 vs 0.2 ± 0.4 , p<0.001).

Higher cortical lesion load at diagnosis is associated with increased CSF neurofilament light chain protein levels

Significantly increased CSF NF-L protein was found in the TS-MSlow (fold change=1.9, p=0.003) and TS-MShigh (fold change=3.97, p≤0.001) patients compared to controls (Fig 3C). CSF NF-L was also increased in the TS-MShigh group compared to the TS-MSlow group (fold change=2.3, p≤0.001) (Fig 3C). Furthermore, we found a significant correlation between the CSF protein level of NF-L and both the volume (r=0.406; p=0.015) and the number of cortical lesions (r=0.421; p=0.011), but not with T2-WMLV (r=-0.046; p=0.716).

Higher cortical lesion load at MS diagnosis is associated with increased pro-inflammatory CSF cytokine and chemokine expression

The protein levels of TNF, sTNFR1, IFN γ , CXCL12, CXCL13, IL6, IL8, IL-10, BAFF, APRIL, LIGHT, TWEAK, MMP-2, Pentraxin3 and sCD163 were increased in the CSF of the TS-MShigh group compared to both control and TS-MSlow groups (FDR < 0.05) (Fig 4). Only the protein levels of IFN- α 2, IFN- λ 2 and CCL25 were significantly increased in the TS-MSlow group compared to both control and TS-MShigh groups. To address the specificity and sensitivity of individual molecules as biomarkers in classifying patients into MSlow and MShigh, we performed the ROC curve analysis (Supplementary Table 3): all these 18 molecules showed a very good classification performance (AUC ≥ 0.80).

Validation of biomarker candidates using an independent cohort of MS patients

The association between CSF NF-L and cortical lesion load found in the TS was validated in the independent VS cohort. An increased NF-L protein expression was also found in VS-MSlow (fold change=2.4, p=0,049) and VS-MShigh patients (fold change=5.4, p<0.0001) compared to controls, and in VS-MShigh compared to VS-MSlow (fold change=2.2, p=0.0005) (Fig 3C).

All molecules found to be differentially expressed between TS-MShigh and TS-MSlow were also differentially expressed between VS-MSlow and VS-MShigh groups in our validation analysis, with the exception of IL6 and TWEAK (Fig 4). Specificity, sensitivity and accuracy in

classifying cases with a high cortical lesion load and intrathecal inflammation was obtained by ROC analysis of these 18 molecules: except for TWEAK and IL-6, all the other molecules showed a good accuracy in classifying cases in this way ($AUC \geq 0.70$, Supplementary Table 3).

In agreement with the training set results, the classification of the validation set into VS-MSlow and VS-MShigh did not change when the intracortical lesions alone when used to classify the patients.

Comparison of the post-mortem and patient studies.

Among all the molecules analysed from the post-mortem and clinical cohorts, TNF, IFN γ , CXCL13 and IL10 were commonly increased in the CSF of PM-MShigh compared to PM-MSlow, TS-MShigh compared to TS-MSlow and in VS-MShigh compared to VS-MSlow groups (Fig 5A). In addition, TNF, IFN γ and CXCL13 gene expression were correspondingly found upregulated in the meninges of the PM-MShigh compared to PM-MSlow group (Fig 5). Together these three molecules show a good association (specificity 80%, sensitivity 100%) with the outcome VS-MShigh vs VS-MSlow. Moreover, a linear multivariate model was developed (Table 3) containing as independent variables IFN γ , TNF, CXCL12, CXCL13, IL6, IL10 and LIGHT, which demonstrates that these variables explain 89% of the variance in cortical lesion volume ($n=39$, R^2 0.8856, $p<0.0001$) and 87% of the variance in cortical lesion number ($n=39$, R^2 0.876, $p<0.0001$). There were no significant variables that could predict T2WMLV (data not shown). Furthermore, we found that the three cytokines that were elevated in the post-mortem meninges and CSF and in both patient groups, namely TNF, IFN γ and CXCL13 explained in turn 88% (0.7824/0.8856) of the variance explained by the 7 cytokine model for cortical lesion number (Fig 6A) and 86% (0.7511/0.8752) of the variance for cortical lesion volume (Fig 6B).

DISCUSSION

We have identified an intrathecal (meninges and CSF) inflammation profile in a post-mortem MS cohort that is defined by high levels of GM demyelination and meningeal inflammation. The molecular pattern of increased CSF pro-inflammatory cytokines and chemokines (TNF, LT α , IFN γ , IL2, IL10, IL12p40, IL16, CXCL10, CXCL13, CXCL20, CCL17 and CCL22) was associated with increased meningeal inflammation and GM demyelination and, in addition, early disability onset and age at death. The finding of increased intrathecal levels of molecules associated with B cell recruitment and activity (CXCL13, CXCL10, IL6, IL10, TNF and LT α),

together with their increased gene expression, in the subgroup of post-mortem MS patients with high meningeal inflammation and cortical GM demyelination, strongly suggests a link between the degree of the compartmentalized meningeal immune response and both the underlying cortical pathology and a more rapid disease evolution. The lack of tight junctions in cells lining the pial membrane, damage to the glia limitans caused by the inflammation⁵ and a degree of continuity between the subarachnoid and perivenular spaces would allow proteins derived from circulating CSF to easily reach the underlying GM⁴¹. Due to the similarity between the changes in mRNA levels in the meninges and protein levels in the CSF, we suggest that immune cells in the subarachnoid space, whether diffuse or focally organized, release inflammatory/cytotoxic mediators into the CSF, creating an intracerebral milieu that sustains chronic compartmentalized inflammation and, at the same time, directly mediates and/or exacerbates cortical pathology and disease progression⁴¹. It was not possible to include in our study post-mortem CSF samples from cases of non-MS CNS inflammatory conditions, so we cannot say at this stage that the clear association between the particular combination of cytokines and chemokines and the underlying cortical pathology is specific to MS.

In order to determine whether the post-mortem CSF profiles are present at earlier stages in the disease process, we analysed the intrathecal immune profile associated with increased cortical pathology at the time of diagnosis of two independent groups of MS patients. The groups of MS patients with increased GM damage on MRI showed a remarkably similar, but not identical, CSF profile when compared to the post mortem samples with increased GM demyelination, even at this early stage of disease. This is in agreement with the observation of substantial meningeal infiltrates and subpial demyelination in cortical biopsies of patients at the early stages of disease¹¹. Even the protein levels in vivo were quantitatively similar to those observed in the post-mortem samples. In particular, a combination of pro-inflammatory cytokines (TNF, IFN γ , IL6) and molecules involved in lymphoid-neogenesis (CXCL12, CXCL13, TNF) and B-cell and plasma cell/blast activity (IL6, IL10, TNF, BAFF, APRIL, LIGHT, TWEAK) defined those subjects with the most extensive GM demyelination. The further analysis of CSF from an independent unbiased cohort of MS patients with an heterogeneous degree of disease severity, who were consecutively enrolled in the neurology clinic at the time of diagnosis, identified an almost identical cytokine/chemokine profile, thus validating and increasing confidence in our findings. The elevated CSF expression of major inflammatory molecules, such as TNF, IFN γ , BAFF, IL6 and IL8, suggests the presence of an elevated involvement of multiple immune cell populations, including T lymphocytes and monocytes, indicating an increased inflammatory activity that probably characterizes patients with increased cortical pathology and a more progressive clinical disease. In addition, the different

immune populations contributing to the intracerebral inflammatory activity might also have an important role in the activation and regulation of the B-cell and plasma blast functions.

In contrast, although less well defined, a different inflammatory profile associated with innate and myeloid immunity (type I and III IFNs) and Th2 regulatory molecules (CCL25), was observed in the CSF of MS patients with low GM lesion number and volume. This suggests that the balance of inflammatory mechanisms in this patient group is altered towards the downregulation of pro-inflammatory pathways. In this context, the increase in gene expression for IL17 in the post-mortem meninges of MS cases with only low levels of inflammation and demyelination was somewhat surprising given its role in promoting meningeal inflammation in mice⁵¹ and points towards a possible immunoregulatory role in this compartment in progressive MS. However, no significant difference was seen in the levels of IL17 protein in the post-mortem CSF and it was not included in the multiplex analysis of the patients samples. Further investigations are thus required to understand the role of IL17 in progressive disease.

It is intriguing that such a CSF profile includes high levels of molecules linked to B cell recruitment and maintenance in the CNS (CXCL13 and CXCL12) as well as mediators related to B cell immune functions (IL6, IL10, TNF, BAFF, APRIL, TWEAK) at this early stage of the disease evolution. This supports a key role for a compartmentalized B cell and plasma cell/blast response in the pathogenesis of GM damage at least in a subgroup of patients from an early stage^{14,42,43}. Such data reinforces the idea that the immune response is compartmentalised and may help to explain why most of the immunomodulatory drugs are ineffective in progressive MS^{44,45} as they do not efficiently access this compartment. Our observations are also in line with previous studies^{6,17,29,42,46,47} and confirm the key role of a compartmentalized adaptive immune response that specifically mediates and exacerbates the pathology of the adjacent cerebral cortex in MS. The finding of specific individual CSF/MRI profiles linked to the degree of meningeal inflammation and cortical lesion load at the time of the diagnosis suggests that a specific differential involvement of intrathecal inflammatory responses, possibly compartmentalized in ectopic lymphoid-like structures, and of GM demyelination might be linked to long term disease evolution.

To confirm that the patient group with a higher cortical lesion load on MRI (TS-MShigh) are characterized by a more severe GM damage we have also evaluated the global cortical thickness (a general proxy of GM atrophy) and the levels of NF-L in the CSF. Both these parameters clearly, suggest that the inflammatory and neurodegenerative processes within the GM are significantly more aggressive in patients with a higher cortical lesion load, as previously suggested by a number of imaging studies⁹. They also confirm previous neuropathological findings of increased axonal and neuronal loss in subpial GM lesions of MS patients with increased levels of meningeal

inflammation and more rapid disease progression^{5,6,14,18} suggesting that intrathecal inflammatory milieu may be one of the key determinant of the rate of cortical neurodegeneration in MS.

The combined post-mortem and patient results suggest that cortical damage in MS is associated with a specific inflammatory intrathecal profile that is already detectable at disease onset, persists throughout the entire disease course, and can be still detected at the final stage of the disease in the post-mortem brain, although further longitudinal studies are necessary to substantiate this idea. Moreover, these data point out the crucial value of the CSF analysis, suggesting that it might be possible to identify MS patients at high risk of severe GM damage already at the point of diagnosis by a specific combined CSF and MRI profile. Finally, the association of both severe GM damage and meningeal inflammation with a more rapidly progressing disease, as observed by several imaging⁸ and post-mortem studies^{6,11,14,17}, also confirms the possible prognostic value of such data and the possibility to stratify patients for more appropriate treatment options already at diagnosis. In particular, the panel of molecules commonly identified in both the neuropathological and clinical arms of the study (CXCL13, IL10, TNF and IFN γ) might represent a useful prognostic signature of cortical damage and meningeal inflammation, linked to a more rapid and severe disease progression.

The fact that the classification into two MS subgroups with substantially different cortical lesion load at diagnosis was also confirmed when only intracortical lesions alone were used to classify the patients. This strongly supports the existence of a “cortical variant” of multiple sclerosis in which the cerebral cortex is predominantly or exclusively involved⁴⁸.

Although four different experiments have been conducted to increase the reliability of our data, this study is not without limitations. We see the low sensitivity of MRI methodologies in detecting all cortical lesions in vivo to be a limitation, although comparative neuropathological and in vivo studies have suggested that the load of detectable MRI cortical lesions is well correlated with the total number of cortical lesions observed by neuropathological assessments, including the most numerous sub-pial type III cortical lesions^{49,50}. Nevertheless, to overcome this limitation and to identify patients with a more severe cortical pathology, we also included in our analysis a reliable evaluation of cortical thickness and of CSF NF-L as additional markers of GM damage. Moreover, we have analysed post-mortem tissues applying the same criteria (cases are differentiated according to cortical lesion load) used for the MS patients. As the examined post-mortem MS population was made up of SPMS cases, the level of cortical demyelination is of course substantially more severe than the one detected in RRMS patients at diagnosis by 3T-MRI methodology. However, such a combined analysis used in this study still suggests that it may be possible to stratify MS patients according to the GM lesion load and inflammatory profile at any disease stage.

A further limitation of this study may be the stringent biostatistical analyses performed, which might have underestimated the number of significant biomarkers. Extending this study to a larger MS population could help to identify a more complex and complete panel of CSF biomarkers associated with cortical damage and intrathecal inflammation. Finally, the lack of a clinical follow up at this stage has necessitated the use of several surrogate markers of disease severity to indicate the development of an early and severe GM damage. Therefore, longitudinal studies are required to confirm, *in vivo*, that the CSF profile associated with the severe GM damage can be used as a prognostic marker of disease evolution.

In conclusion, our analysis has identified a set of inflammatory mediators in patient CSF captured at diagnosis, which reflects the state of meningeal inflammation and the extent of cortical damage, which is comparable to that seen post-mortem in neuropathologically characterised MS. The similarity of such a CSF profile with that observed at death in more rapidly progressive MS cases, strongly reinforces a potential key role of CSF analysis at disease onset and indicates its possible utility as a prognostic marker for MS course from the early phase of the disease. Since modern advanced imaging techniques are not yet able to specifically identify and quantify meningeal inflammation¹⁶ and subpial demyelination, we propose the combined CSF and MRI profiling of the MS patients at diagnosis will be an appropriate *in-vivo* surrogate of meningeal and intrathecal inflammation and might help to define other different specific MS phenotypes related to the characteristic heterogeneity of the disease and subsequently to select the most appropriate treatment.

Acknowledgements: We would like to thank the technical support from the Complex Protein Mixture (CPM) Facility at Istituto Superiore di Sanità, Rome, Italy. We would like to acknowledge Dr. Damiano Marastoni and Dr. Valentina Mazziotti for the useful assistance in selecting CSF samples from the examined controls. We acknowledge the UK MS Society Tissue Bank for the supply of post-mortem tissue and CSF samples. Dr Magliozzi was supported by the GR-2010-2313255 grant from Italian Ministry of Health and from the Italian MS Foundation (FISM 16/17/F14). Prof Calabrese was supported by the GR-2013-02-355322 grant from Italian Ministry of Health. Prof. Reynolds and Prof. Nicholas were supported by the MS Society (the UK MS Society Tissue Bank, grant no 007/14) and the Imperial College NIHR Biomedical Research Centre. This study was specifically supported by a Progressive Multiple Sclerosis Alliance grant (PA 0124) to M. Calabrese, R. Reynolds and O. Howell.

Author Contributions:

RM, OH, RR and MC contributed to the conception and design of the study; RM, OH, RN, CC, MC, CR, SR, FF and SM contributed to the acquisition and analysis of data; RM, OH, RR, MC, MP, MDB, AG, FBP, SM, SR, RC, AB and SM contributed to drafting the text

Potential Conflicts of Interest

There are no conflicts of interest related to this study.

References

1. Graumann U, Reynolds R, Steck AJ, Schaeren-Wiemers N. Molecular changes in normal appearing white matter in multiple sclerosis are characteristic of neuroprotective mechanisms against hypoxic insult. *Brain Pathol.* 2003;13(4):554–73.
2. Howell OW, Rundle JL, Garg A, et al. Activated Microglia Mediate Axoglial Disruption That Contributes to Axonal Injury in Multiple Sclerosis. *J. Neuropathol. Exp. Neurol.* 2010;69(10):1017-1033.
3. Kutzelnigg A, Lucchinetti CF, Stadelmann C, et al. Cortical demyelination and diffuse white matter injury in multiple sclerosis. *Brain* 2005;128(Pt11):2705-12.
4. Chard D, Miller D. Grey matter pathology in clinically early multiple sclerosis: Evidence from magnetic resonance imaging. *J. Neurol. Sci.* 2009;282(1-2):5–11.
5. Magliozzi R, Howell OW, Reeves C, et al. A Gradient of neuronal loss and meningeal inflammation in multiple sclerosis. *Ann. Neurol.* 2010;68(4):477-493.
6. Howell OW, Reeves CA, Nicholas R, et al. Meningeal inflammation is widespread and linked to cortical pathology in multiple sclerosis. *Brain* 2011;134(Pt9):2755-71.
7. Fisniku LK, Chard DT, Jackson JS, et al. Gray matter atrophy is related to long-term disability in multiple sclerosis. *Ann. Neurol.* 2008;64(3):247-54.
8. Calabrese M, Poretto V, Favaretto A, et al. Cortical lesion load associates with progression of disability in multiple sclerosis. *Brain* 2012;135(Pt10):2952–61.
9. Filippi M, van den Heuvel MP, Fornito A, et al. Assessment of system dysfunction in the brain through MRI-based connectomics. *Lancet Neurol.* 2013;12(12):1189-99.
10. De Stefano N, Guidi L, Stromillo ML, et al. Imaging neuronal and axonal degeneration in multiple sclerosis. *Neurol. Sci.* 2003;24(S5):s283–s286.
11. Lucchinetti CF, Popescu BF, Bunyan RF, et al. Inflammatory Cortical Demyelination in Early Multiple Sclerosis. *N. Engl. J. Med.* 2011;365(23):2188-97.
12. Ransohoff RM, Kivisäkk P, Kidd G. Three or more routes for leukocyte migration into the central nervous system. *Nat. Rev. Immunol.* 2003;3(7):569–581.
13. Serafini B, Rosicarelli B, Magliozzi R, et al. Detection of ectopic B-cell follicles with germinal centers in the meninges of patients with secondary progressive multiple sclerosis. *Brain Pathol.* 2004;14(2):164–174.

14. Magliozzi R, Howell O, Vora A, et al. Meningeal B-cell follicles in secondary progressive multiple sclerosis associate with early onset of disease and severe cortical pathology. *Brain* 2007;130(Pt4):1089-1104.
15. Gardner C, Magliozzi R, Durrenberger PF, et al. Cortical grey matter demyelination can be induced by elevated pro-inflammatory cytokines in the subarachnoid space of MOG-immunized rats. *Brain* 2013;136(Pt12):3596-608.
16. Absinta M, Cortese ICM, Vuolo L, et al. Leptomeningeal gadolinium enhancement across the spectrum of chronic neuroinflammatory diseases. *Neurology* 2017;88(15):1439–1444.
17. Haider L, Zrzavy T, Hametner S, et al. The topography of demyelination and neurodegeneration in the multiple sclerosis brain. *Brain* 2016; 139(Pt3):807-15.
18. Androdias G, Reynolds R, Chanal M, et al. Meningeal T cells associate with diffuse axonal loss in multiple sclerosis spinal cords. *Ann. Neurol.* 2010;68(4):465-476.
19. Howell OW, Schulz-Trieglaff EK, Carassiti D, et al. Extensive grey matter pathology in the cerebellum in multiple sclerosis is linked to inflammation in the subarachnoid space. *Neuropathol. Appl. Neurobiol.* 2015; 41(6):798-813.
20. Choi SR, Howell OW, Carassiti D, et al. Meningeal inflammation plays a role in the pathology of primary progressive multiple sclerosis. *Brain* 2012; 135(Pt 10):2925-37.
21. Geurts JJ, Bö L, Pouwels PJ, et al. Cortical lesions in multiple sclerosis: Combined postmortem MR imaging and histopathology. *Am. J. Neuroradiol.* 2005; 26(3):572-7.
22. Seewann A, Vrenken H, Kooi EJ, et al. Imaging the tip of the iceberg: visualization of cortical lesions in multiple sclerosis. *Mult. Scler.* 2011;17(10):1202–1210.
23. Calabrese M, De Stefano N, Atzori M, et al. Detection of cortical inflammatory lesions by double inversion recovery magnetic resonance imaging in patients with multiple sclerosis. *Arch. Neurol.* 2007;64(10):1416–22.
24. Seewann A, Kooi E-J, Roosendaal SD, et al. Postmortem verification of MS cortical lesion detection with 3D DIR. *Neurology* 2012;78(5):302–8.
25. Sethi V, Yousry TA, Muhlert N, et al. Improved detection of cortical MS lesions with phase-sensitive inversion recovery MRI. *J. Neurol. Neurosurg. Psychiatry* 2012; 83(9):877-82.
26. Kilsdonk ID, de Graaf WL, Soriano AL, et al. Multicontrast MR imaging at 7T in multiple sclerosis: Highest lesion detection in cortical gray matter with 3D-FLAIR. *AJNR Am. J. Neuroradiol.* 2013;34(4):791–6.

27. Filippi M, Evangelou N, Kangarlu A, et al. Ultra-high-field MR imaging in multiple sclerosis. *J. Neurol. Neurosurg. Psychiatry* 2014;85(1):60–6.
28. Petzold A, Steenwijk MD, Eikelenboom JM, et al. Elevated CSF neurofilament proteins predict brain atrophy: A 15-year follow-up study. *Mult. Scler.* 2016;22(9):1154–62.
29. Krumbholz M, Theil D, Cepok S, et al. Chemokines in multiple sclerosis: CXCL12 and CXCL13 up-regulation is differentially linked to CNS immune cell recruitment. *Brain* 2006; 129(Pt 1):200–11.
30. Sharief MK, Hentges R. Association between tumor necrosis factor-alpha and disease progression in patients with multiple sclerosis. *N. Engl. J. Med.* 1991;325(7):467–72.
31. Baraczka K, Nékám K, Pozsonyi T, et al. Investigation of cytokine (tumor necrosis factor-alpha, interleukin-6, interleukin-10) concentrations in the cerebrospinal fluid of female patients with multiple sclerosis and systemic lupus erythematosus. *Eur. J. Neurol.* 2004;11(1):37–42.
32. Duan H, Luo Y, Hao H, et al. Soluble CD146 in cerebrospinal fluid of active multiple sclerosis. *Neuroscience* 2013; 235:16–26.
33. Lovato L, Willis SN, Rodig SJ, et al. Related B cell clones populate the meninges and parenchyma of patients with multiple sclerosis. *Brain* 2011;134(Pt 2):534–41.
34. Polman CH, Reingold SC, Banwell B, et al. Diagnostic criteria for multiple sclerosis: 2010 Revisions to the McDonald criteria. *Ann. Neurol.* 2011;69(2):292–302.
35. Durrenberger PF, Fernando S, Kashefi SN, et al. Effects of antemortem and postmortem variables on human brain mRNA quality: a BrainNet Europe study. *J. Neuropathol. Exp. Neurol.* 2010;69(1):70–81.
36. Teunissen CE, Petzold A, Bennett JL, et al. A consensus protocol for the standardization of cerebrospinal fluid collection and biobanking. *Neurology* 2009;73(22):1914–22.
37. Geurts JJ, Roosendaal SD, Calabrese M, et al. Consensus recommendations for MS cortical lesion scoring using double inversion recovery MRI. *Neurology* 2011;76(5):418–24.
38. Pham DL, Prince JL. Adaptive fuzzy segmentation of magnetic resonance images. *IEEE Trans. Med. Imaging* 1999;18(9):737–52.
39. Avants BB, Tustison NJ, Song G, et al. A reproducible evaluation of ANTs similarity metric performance in brain image registration. *Neuroimage* 2011;54(3):2033–44.
40. Schmidt P, Gaser C, Arsic M, et al. An automated tool for detection of FLAIR-hyperintense

- white-matter lesions in Multiple Sclerosis. *Neuroimage* 2012;59(4):3774–83.
41. Calabrese M, Magliozzi R, Ciccarelli O, et al. Exploring the origins of grey matter damage in multiple sclerosis. *Nat. Rev. Neurosci.* 2015;16(3):147–158.
 42. Corcione A, Casazza S, Ferretti E, et al. Recapitulation of B cell differentiation in the central nervous system of patients with multiple sclerosis. *Proc. Natl. Acad. Sci. U. S. A.* 2004;101(30):11064–9.
 43. Haas J, Bekeredjian-Ding I, Milkova M, et al. B cells undergo unique compartmentalized redistribution in multiple sclerosis. *J. Autoimmun.* 2011; 37(4):289-99.
 44. Hauser SL. Multiple lessons for multiple sclerosis. *N. Engl. J. Med.* 2008;359(17):1838–41.
 45. Kappos L, Li D, Calabresi PA, et al. Ocrelizumab in relapsing-remitting multiple sclerosis: a phase 2, randomised, placebo-controlled, multicentre trial. *Lancet* 2011;378(9805):1779–87.
 46. Krumbholz M, Theil D, Derfuss T, et al. BAFF is produced by astrocytes and up-regulated in multiple sclerosis lesions and primary central nervous system lymphoma. *J. Exp. Med.* 2005; 201(2):195-200.
 47. Meinl E, Krumbholz M, Derfuss T, et al. Compartmentalization of inflammation in the CNS: A major mechanism driving progressive multiple sclerosis. *J. Neurol. Sci.* 2008; 274(1-2):42-4.
 48. Zarei M, Chandran S, Compston A, Hodges J; Cognitive presentation of multiple sclerosis: evidence for a cortical variant. *J Neurol Neurosurg Psychiatry* 2003;74(7):872–77.
 49. Bö L, Geurts JJ, Mörk SJ, van der Valk P. Grey matter pathology in multiple sclerosis. *Acta Neurol. Scand. Suppl.* 2006;183:48–50.
 50. Schmierer K, Parkes HG, So P-W, et al. High field (9.4 Tesla) magnetic resonance imaging of cortical grey matter lesions in multiple sclerosis. *Brain* 2010;133(Pt 3):858–67.
 51. Peters A, Pitcher LA, Sullivan JM, et al. Th17 cells induce ectopic lymphoid follicles in central nervous system tissue inflammation. *Immunity* 2011;35:986-996.

Legends

Figure 1

Neuropathological assessment showing the association between meningeal inflammation and grey matter demyelination. In contrast to the PM-MSlow group (A-C, E), the PM-MShigh group was characterized by high degree of meningeal inflammation (A, F-I), particularly enriched in CD20+ B cells and CD3+ T cells (G-I), and high levels of cortical demyelination (B, D, F). A: Quantifying the number of cells per meningeal inflammatory infiltrates in PM-MSlow group (green bars; mean=10.42; SEM=2.48; range= 7-32) compared with the PM-MShigh (red bars; mean=68.83; SEM=7.8; range= 43-167) significant higher meningeal inflammation (fold change: 6.5; $p<0.0001$) was detected in PM-MShigh compared to the PM-MSlow group. B: Quantification of cortical GM demyelination in PM-MSlow group (green bars; median=24.5% + SEM=2.016; range=14-51%) compared with the PM-MShigh group (red bars; median=71% + SEM=1.12; range= 57-82%) revealed significant increased (fold change: 2.9; $p<0.0001$) GM demyelination was found in PM-MShigh compared to the PM-MSlow group. (B; immunostaining for myelin oligodendrocyte glycoprotein in ; MOG) and meningeal cellular infiltrates (D). Scale bars = (C, D) 5 mm; (E, F) 2.5 mm; (G-I) 20 μ m.

Figure 2

Analysis of the changes in levels of inflammatory gene transcripts and proteins in post-mortem meninges and CSF of MS and control cases. Analysis of the presence and levels of inflammatory gene transcripts (A) and protein (B) in the post-mortem meninges (A) and CSF (B) respectively, in 10 controls (yellow bars), 10 PM-MSlow (green bars) and 10 PM-MShigh cases (red bars). Significantly increased expression of gene transcripts (A) and correspondent proteins (B) for CXCL13, TNF, IFN γ , CXCL10, IL2 and CCL22 were found in PM-MShigh cases compared to controls. CXCL13, TNF and CXCL10 gene expression was increased in PM-MShigh compared to PM-MSlow (A), whilst CXCL13, TNF and CCL22 protein expression was increased in the CSF of PM-MShigh compared to PM-MSlow groups (B).

Significantly elevated gene expression for the pro-inflammatory molecules TNF, IFN γ , IL2, IL22, CXCL9, CXCL10, CXCL13, CXCL20 and CCL22 was found in the meninges of the PM-MShigh group compared to controls; IL9 and IL17 gene expression was up-regulated in the PM-MSlow group compared to controls; CXCL9, CXCL10, CXCL13 and TNF genes expression was up-regulated in the meninges of the PM-MShigh group compared to the PM-MSlow group; finally, IL17A gene expression was elevated in the PM-MSlow compared to the PM-MShigh group (A).

Significantly higher protein levels of all the reported molecules in B, except IL-4, were found in the CSF of PM-MShigh compared to controls; only IL-4 was increased in the CSF of PM-MSlow compared to controls (B). When the PM-MShigh cases were compared to the PM-MSlow cases, there was a significant increase in the levels of TNF, LT α , CXCL13, CCL22 and IL12p40 (B). In contrast, only IL4 protein was increased in the CSF of PM-MSlow compared with the control group (B) p values for each statistically significant comparison have been reported (*=p \leq 0.05; **=p \leq 0.01; ***=p \leq 0.001).

Figure 3

Imaging cortical pathology in the MS study cohort. Patients were grouped based on the presence of at least 10 CLs (TS-MShigh) or less than 2 CLs (TS-MSlow). Illustration of MRI profile representative of the T-MSlow group (A) and the T-MShigh subjects (B). 3D Double Inversion Recovery MRI acquisitions are reported in three views: axial, coronal and sagittal, respectively. CLs (red arrows) and WM lesions (green arrows) are highlighted. Protein expression of NF-L in the diagnostic CSF (C) taken from 26 controls (yellow bar), 15 T-MSlow (green bar), 20 T-MShigh (red bar), 19 V-MSlow (green bar with texture) and 19 V-MShigh (red bar with texture) patients. Statistical analysis of the data was performed using the non parametric Mann-Whitney test. p values for each statistically significant comparison are reported (*=p<0.05; **=p \leq 0.01; ***=p<0.001).

Figure 4

CSF protein analysis in MS and control cohorts. Protein levels of the 18 CSF biomarkers found differentially expressed in the CSF of 26 controls (ctrls; yellow bar), 15 TS-MSlow (green bar), 20 TS-MShigh (red bar), 19 VS-MSlow (green bar with texture) and 19 VS-MShigh (red bar with texture) patients. The levels of CXCL13, CXCL12, CCL25, TNF, sTNFR1, IFN γ , IFN- α 2, IFN- λ 2, IL6, IL8, IL-10, BAFF, APRIL, LIGHT, TWEAK, GM-CSF, MMP-2, Pentraxin3 and sCD163 were significantly increased in the CSF of the TS-MShigh and VS-MShigh groups compared to controls (FDR < 0.05). Only the levels of IFN- α 2, IFN- λ 2, CCL25 were significantly elevated in the MSlow groups compared to both controls and MShigh groups. Significant increases in CXCL12, CXCL13, IFN γ , TNF, TNFR1, APRIL, LIGHT and BAFF were also observed in the CSF of TS-MShigh and VS-MShigh compare to TS-MSlow and VS-MSlow groups respectively. Statistical analysis of the data was performed using the non parametric Mann-Whitney test. p values for each statistically significant comparison have been reported (*=p \leq 0.05; **=p \leq 0.01; ***=p \leq 0.001).

Figure 5

Comparison of the post-mortem and in-vivo patient studies.

All differentially expressed inflammatory molecules identified from the post-mortem (meningeal gene expression and CSF protein expression) and clinical studies (CSF protein expression in the training and validation MS cohorts) are shown (A) to highlight the immune mediators that best reflect a state of increased cortical pathology at both diagnosis and post-mortem. In both the studies, the molecules overexpressed in MS_{low} groups are shown in green, while the molecules overexpressed in MS_{high} groups are shown in red. Molecules overexpressed only in the post-mortem or in the in-vivo group of patients are represented in yellow. TNF, IFN γ , CXCL13 and IL10 (black arrows) were found overexpressed in the CSF of both PM-MS_{high} (compared to PM-MS_{low}) and in TS-MS_{high} and in VS-MS_{high} (compared to TS-MS_{low} and VS-MS_{low}). In addition, the TNF, IFN γ and CXCL13 gene expression was found correspondingly upregulated in the meninges of PM-MS_{high} compared to PM-MS_{low}.

Figure 6

Predicting model of cortical damage.

Influence of each cytokine on the chance of cortical lesions (A) and volume (B) in the in-vivo examined MS populations: TNF, IFN γ , CXCL13 might explain 88% of cortical lesion number (A) and 85% of cortical lesion volume (B).

Table 1: Demographic and clinical characteristics of the post-mortem cases.

Cases	Sex	Age at Death	Cause of death	PM interval (hrs)	
C5	F	95	Bronchopneumonia	9	CSF and meningeal analysis
C7	F	85	Oesophageal cancer	9	CSF and meningeal analysis
C8	F	93	Bronchopneumonia,	9	Meningeal analysis only
C25	M	35	Tongue carcinoma	22	Meningeal analysis only
C28	F	60	Ovarian cancer	13	Meningeal analysis only
C30	M	75	Bronchopneumonia	17	CSF and meningeal analysis
C32	M	88	Prostate cancer	12	CSF and meningeal analysis
C36	M	68	Heart failure	30	CSF and meningeal analysis
C45	M	77	Myocardial degeneration	22	Meningeal analysis only
C50	M	32	Haeman-giopericytoma	6	CSF and meningeal analysis
C54	M	66	Pancreatic Cancer	16	CSF and meningeal analysis
PDC22	M	75	Lung carcinoma	10	CSF analysis only
PDC32	F	91	Colon cancer	12	CSF analysis only
PDC36	F	57	Breast cancer	15	Used for CSF
MS104	M	53	Multiple sclerosis	12	pm-MS1 (meninges + CSF)
MS296	M	59	Multiple sclerosis	22	pm-MS1 (meninges + CSF)
MS301	F	62	Septicaemia	16	pm-MS1 (meninges only)
MS304	M	52	Pulmonary embolism	13	pm-MS1 (meninges + CSF)
MS311	F	45	Pneumonia	22	pm-MS1 (meninges only)
MS318	F	59	Multiple sclerosis	13	pm-MS1 (meninges + CSF)
MS326	M	62	Multiple sclerosis	24	pm-MS1 (meninges only)
MS347	M	50	Pancreatic carcinoma	13	pm-MS1 (meninges + CSF)
MS364	F	56	Bronchopneumonia	14	pm-MS1(CSF only)
MS376	F	58	Multiple sclerosis	19	pm-MS1 (meninges only)
MS422	M	58	Bronchopneumonia	25	pm-MS1 (CSF only)
MS444	M	49	Renal failure	18	pm-MS1(CSF only)
MS461	M	43	Bronchopneumonia	13	pm-MS1(CSF only)
MS485	F	57	Bronchopneumonia	24	pm-MS1(CSF only)
MS491	F	64	Anaphylactic reaction	9	pm-MS1 (meninges only)
MS402	M	46	Multiple sclerosis	12	pm-MS2 (meninges + CSF)
MS407	F	44	Septicaemia	22	pm-MS2 (meninges + CSF)
MS408	M	39	Pneumonia	21	pm-MS2 (meninges + CSF)
MS423	F	54	Pneumonia	11	pm-MS2 (meninges + CSF)
MS438	F	53	Multiple sclerosis	17	pm-MS2 (meninges + CSF)
MS473	F	40	Bronchopneumonia	9	pm-MS2 (meninges + CSF)
MS497	F	60	Aspiration pneumonia	45	pm-MS2 (meninges + CSF)
MS510	F	38	Pneumonia	19	pm-MS2(meninges only)
MS513	M	51	Multiple sclerosis	17	pm-MS2 (meninges + CSF)
MS517	F	48	Chest sepsis	12	pm-MS2 (CSF only)
MS527	M	46	Pneumonia	10	pm-MS2 (meninges only)
MS528	F	45	Multiple sclerosis	17	pm-MS2 (CSF only)

Abbreviations= DisDur: disease duration; AgeWC: age at wheelchair use (EDSS 7); PM interval: post-mortem interval; CSF: cerebrospinal fluid; N.A.: not available; N.W.: not wheelchair bound; N.U.: not used as not presenting with neuropathological features of interest.

Table 2. Demographics and disease characteristics of the MS subjects

Group	Post-mortem (PM)		Patient Test set (TS)		Patient Validation set (VS)	
	Low (15)	High (12)	Low (15)	High (20)	Low (19)	High (19)
MS damage						
Age studied (mean±SD)	55±6.34	45.8±5.42	38.4±11.3	33.2±11.1	35.0±11.1	32.5±10.6
Gender (f:m)	7:8	7:5	10:5	15:5	11:8	12:7
Disease duration (mean±SD years)	24.0±8.5	21.1±6.1	2.1±2.4	3.3±2.0	2.1±2.3	3.2±2.4
EDSS at recruitment (range)			1.5 (1.0-3.5)	2.0 (1.0-4.0)	1.0 (1.0-3.5)	2.0 (1.5-4.5)
Mono/poly symptomatic onset/not available	4/4/7	6/1/4	15/0/0	15/5/0	17/2/0	16/3/0
OCBs Positive/negative /not available	4/0/11	3/0/9	12/3/0	18/2/0	13/6/0	16/3/0
IgG index	N.A.	N.A.	0.61±0.15	0.78±0.25	0.82±0.42	1.08±0.49
PM GM damage assessment (mean±SD)	28.43% ± 11.04	70.03% ± 6.34	-	-	-	-
CLs volume (mm ³ -range)	-	-	49 ± 74 (0-188)	1713 ± 663 (877-2678)	187 ± 204 (0-575)	1579 ± 774 (791-3910)
CLs number (mean±SD)	-	-	0.3 ± 0.5 (0-1)	16.8 ± 6.4 (10-29)	1.9 ± 2.0 (0-5)	11.4 ± 2.5 (8-16)
CTh (mm; range)	-	-	2.72 ± 0.41 (2.45-3.15)	2.53 ± 0.34 (2.31-2.99)	2.83 ± 0.25 (2.54-3.12)	2.62 ± 0.31 (2.34-3.01)
T2WMLV (cm ³ ; range)	-	-	4.7±1.6 (1.4-7.2)	5.6±1.6 (3.1-8.4)	5.2 ±1.9 (2.5-8.4)	6.3±1.8 (3.4-9.2)

Abbreviations: EDSS: Expanded Disability Status Scale; OCB: oligoclonal bands; IgG index: immunoglobulin-G index; PM: post-mortem; GM: grey matter; CL: cortical lesion; CTh: cortical thickness; T2WMLV: T2 white matter lesion volume; N.A.: not available.

Table 3. Models predicting the cortical lesion volume and number using 8 cytokines.

Variable estimate (95% CI lower, upper, p value)	Model	
	Cortical lesion volume (R^2 0.8856)	Cortical lesion number (R^2 0.8752)
IFN γ	26.4769 (9.5229, 43.4308, p=0.003)	0.3437 (0.1840, 0.5034, p=9.38e ⁻⁰⁵)
TNF	4.9407 (0.6130, 9.2684, p=0.0263)	0.0362594 (-0.0045, 0.0770, p=0.0797)
CXCL13	12.900 (6.7815, 19.0187, p=0.00012)	0.1334 (0.0758, 0.1911, p=3.39e ⁻⁰⁵)
CXCL12	0.2720 (0.1071, 0.4369, p=0.00187)	0.0024 (0.0009, 0.0040, p=0.00324)
IL6	42.7753 (18.2392, 67.3114, p=0.0011)	0.4087 (0.1776, 0.6398, p=0.00095)
IL10	-52.2696 (-92.1966, -12.3425, p=0.0116)	-0.3869 (-0.7629, -0.0108, p=0.044)
LIGHT	0.2677 (0.1249, 0.4105, p=0.0005)	0.0025 (0.0011, 0.0039, p=0.00053)

Models predicting the cortical lesion volume and number using 8 cytokines which demonstrates that these molecules may explain 89% of the variance in predicting CL volume (n=39, R^2 0.8856, p<5.057e-16) and 87% of the variance in CL number (n=39, R^2 0.8752, p<2.689e-15).

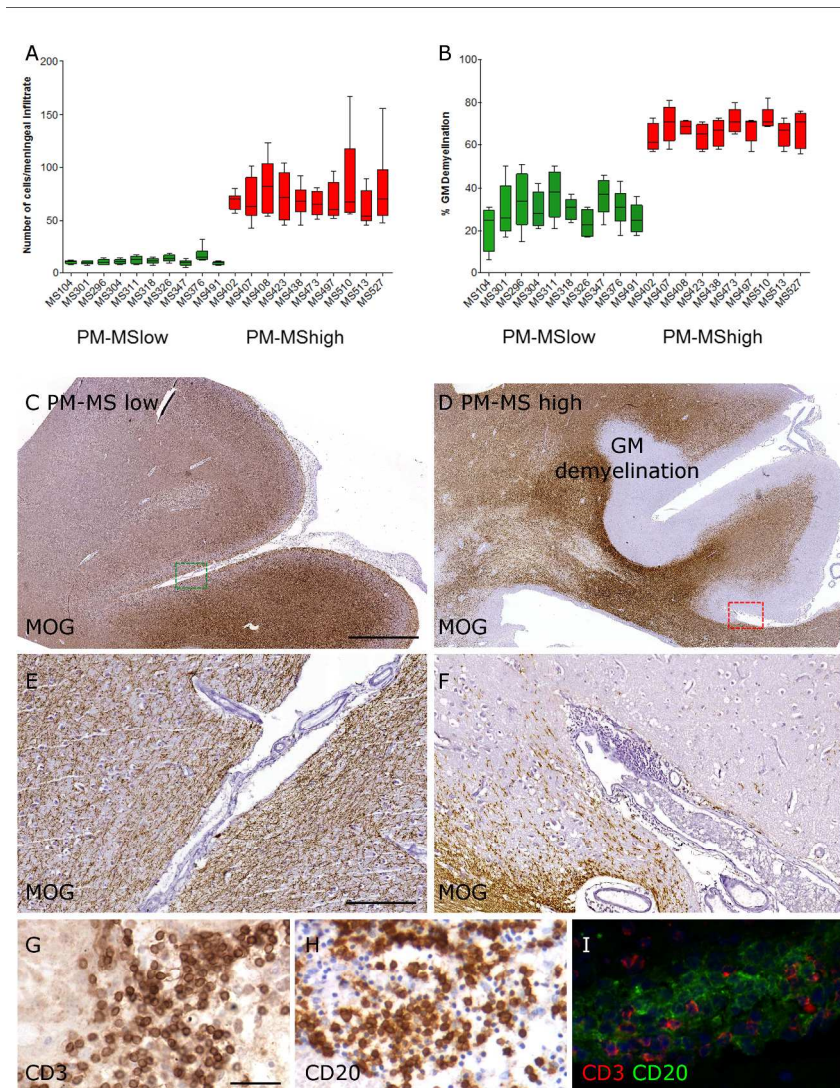


Figure 1

Neuropathological assessment showing the association between meningeal inflammation and grey matter demyelination. In contrast to the PM-MSlow group (A-C, E), the PM-MShigh group was characterized by high degree of meningeal inflammation (A, F-I), particularly enriched in CD20+ B cells and CD3+ T cells (G-I), and high levels of cortical demyelination (B, D, F). A: Quantifying the number of cells per meningeal inflammatory infiltrates in PM-MSlow group (green bars; mean=10.42; SEM=2.48; range= 7-32) compared with the PM-MShigh group (red bars; mean=68.83; SEM=7.8; range= 43-167) significant higher meningeal inflammation (fold change: 6.5; $p < 0.0001$) was detected in PM-MShigh compared to the PM-MSlow group. B: Quantification of cortical GM demyelination in PM-MSlow group (green bars; median=24.5% + SEM=2.016; range=14-51%) compared with the PM-MShigh group (red bars; median=71% + SEM=1.12; range= 57-82%) revealed significant increased (fold change: 2.9; $p < 0.0001$) GM demyelination was found in PM-MShigh compared to the PM-MSlow group. (B; immunostaining for myelin oligodendrocyte glycoprotein in ; MOG) and meningeal cellular infiltrates (D). Scale bars = (C, D) 5 mm; (E, F) 2.5 mm; (G-

Accepted Article

I) 20 μm .

209x297mm (300 x 300 DPI)

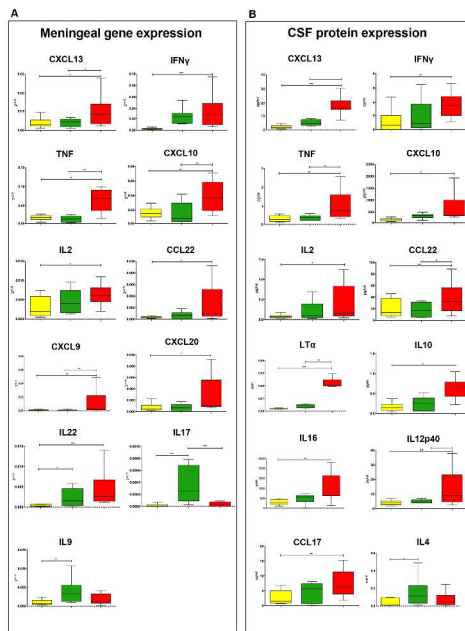


Figure 2

Analysis of the changes in levels of inflammatory gene transcripts and proteins in post-mortem meninges and CSF of MS and control cases. Analysis of the presence and levels of inflammatory gene transcripts (A) and protein (B) in the post-mortem meninges (A) and CSF (B) respectively, in 10 controls (yellow bars), 10 PM-MSlow (green bars) and 10 PM-MShigh cases (red bars). Significantly increased expression of gene transcripts (A) and correspondent proteins (B) for CXCL13, TNF, IFN γ , CXCL10, IL2 and CCL22 were found in PM-MShigh cases compared to controls. CXCL13, TNF and CXCL10 gene expression was increased in PM-MShigh compared to PM-MSlow (A), whilst CXCL13, TNF and CCL22 protein expression was increased in the CSF of PM-MShigh compared to PM-MSlow groups (B).

Significantly elevated gene expression for the pro-inflammatory molecules TNF, IFN γ , IL2, IL22, CXCL9, CXCL10, CXCL13, CXCL20 and CCL22 was found in the meninges of the PM-MShigh group compared to controls; IL9 and IL17 gene expression was up-regulated in the PM-MSlow group compared to controls; CXCL9, CXCL10, CXCL13 and TNF genes expression was up-regulated in the meninges of the PM-MShigh group compared to the PM-MSlow group; finally, IL17A gene expression was elevated in the PM-MSlow compared to the PM-MShigh group (A).

Significantly higher protein levels of all the reported molecules in B, except IL-4, were found in the CSF of PM-MShigh compared to controls; only IL-4 was increased in the CSF of PM-MSlow compared to controls (B).

When the PM-MShigh cases were compared to the PM-MSlow cases, there was a significant increase in the levels of TNF, LT α , CXCL13, CCL22 and IL12p40 (B). In contrast, only IL4 protein was increased in the CSF of PM-MSlow compared with the control group (B) p values for each statistically significant comparison have been reported (*= $p < 0.05$; **= $p < 0.01$; ***= $p < 0.001$).

397x254mm (300 x 300 DPI)

A

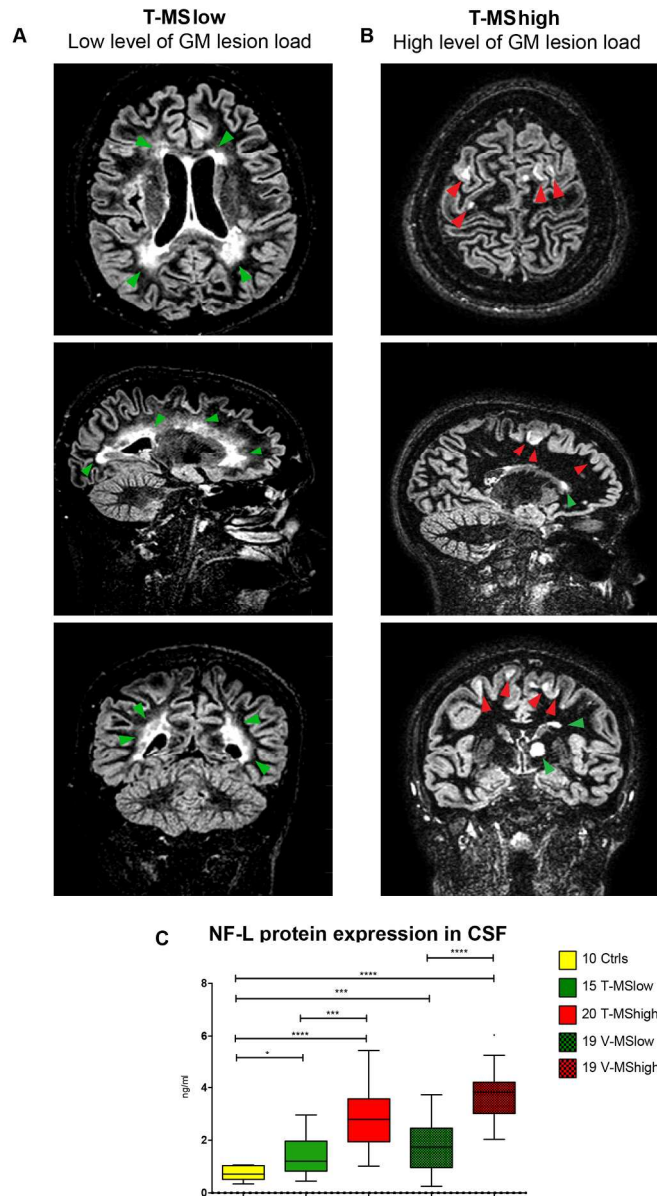


Figure 3

Imaging cortical pathology in the MS study cohort. Patients were grouped based on the presence of at least 10 CLs (T-MShigh) or less than 2 CLs (T-MSlow). Illustration of MRI profile representative of the T-MSlow group (A) and the T-MShigh subjects (B). 3D Double Inversion Recovery MRI acquisitions are reported in three views: axial, coronal and sagittal, respectively. CLs (red arrows) and WM lesions (green arrows) are highlighted. Protein expression of NF-L in the diagnostic CSF (C) taken from 26 controls (yellow bar), 15 T-MSlow (green bar), 20 T-MShigh (red bar), 19 V-MSlow (green bar with texture) and 19 V-MShigh (red bar with texture) patients. Statistical analysis of the data was performed using the non parametric Mann-Whitney test. p values for each statistically significant comparison are reported (*= $p < 0.05$; **= $p < 0.01$; ***= $p < 0.001$).

149x254mm (300 x 300 DPI)

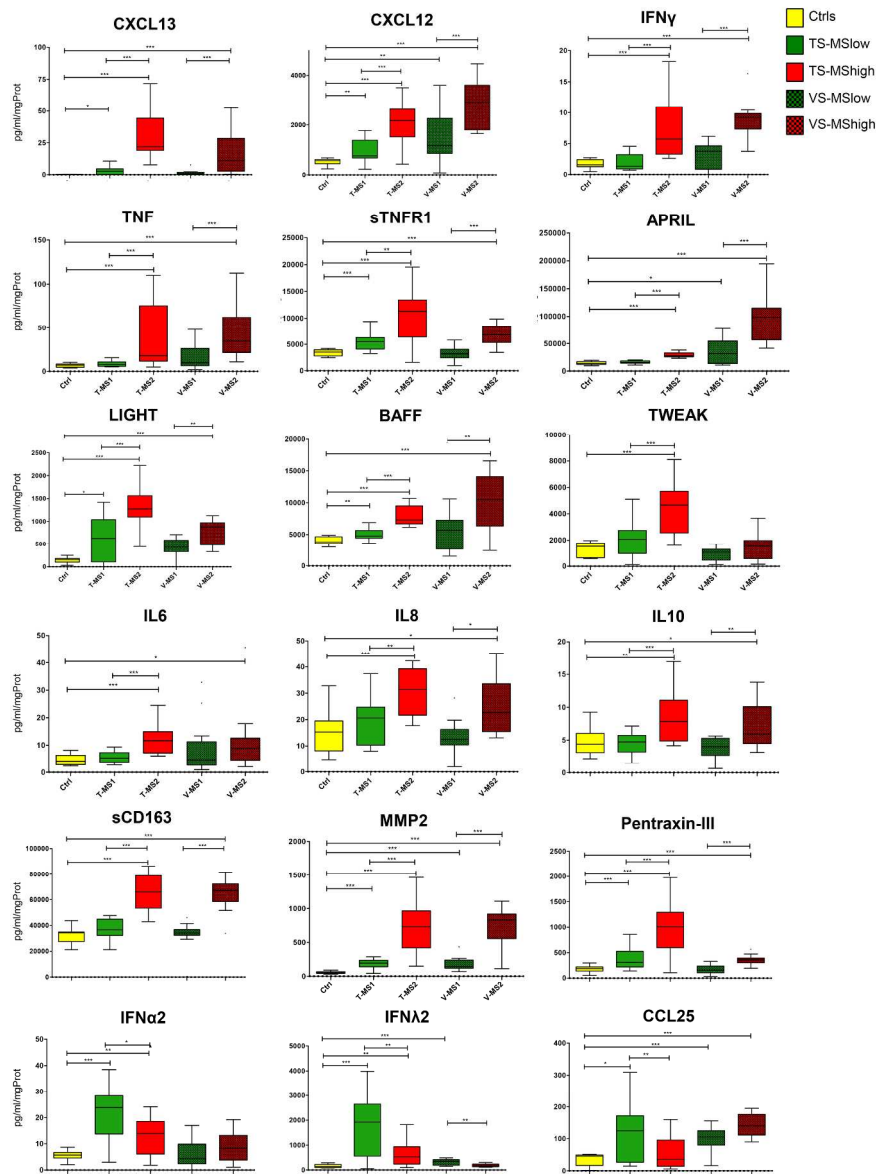


Figure 4

CSF protein analysis in MS and control cohorts. Protein levels of the 18 CSF biomarkers found differentially expressed in the CSF of 26 controls (ctrls; yellow bar), 15 TS-MSlow (green bar), 20 TS-MShigh (red bar), 19 VS-MSlow (green bar with texture) and 19 VS-MShigh (red bar with texture) patients. The levels of CXCL13, CXCL12, CCL25, TNF, sTNFR1, IFN γ , IFN- α 2, IFN- λ 2, IL6, IL8, IL-10, BAFF, APRIL, LIGHT, TWEAK, GM-CSF, MMP-2, Pentraxin3 and sCD163 were significantly increased in the CSF of the TS-MShigh and VS-MShigh groups compared to controls (FDR < 0.05). Only the levels of IFN- α 2, IFN- λ 2, CCL25 were significantly elevated in the MSlow groups compared to both controls and MShigh groups. Significant increases in CXCL12, CXCL13, IFN γ , TNF, TNFR1, APRIL, LIGHT and BAFF were also observed in the CSF of TS-MShigh and VS-MShigh compare to TS-MSlow and VS-MSlow groups respectively. Statistical analysis of the data was performed using the non parametric Mann-Whitney test. p values for each statistically significant comparison have been reported (*=p<0.05; **=p<0.01; ***=p<0.001).

Acc

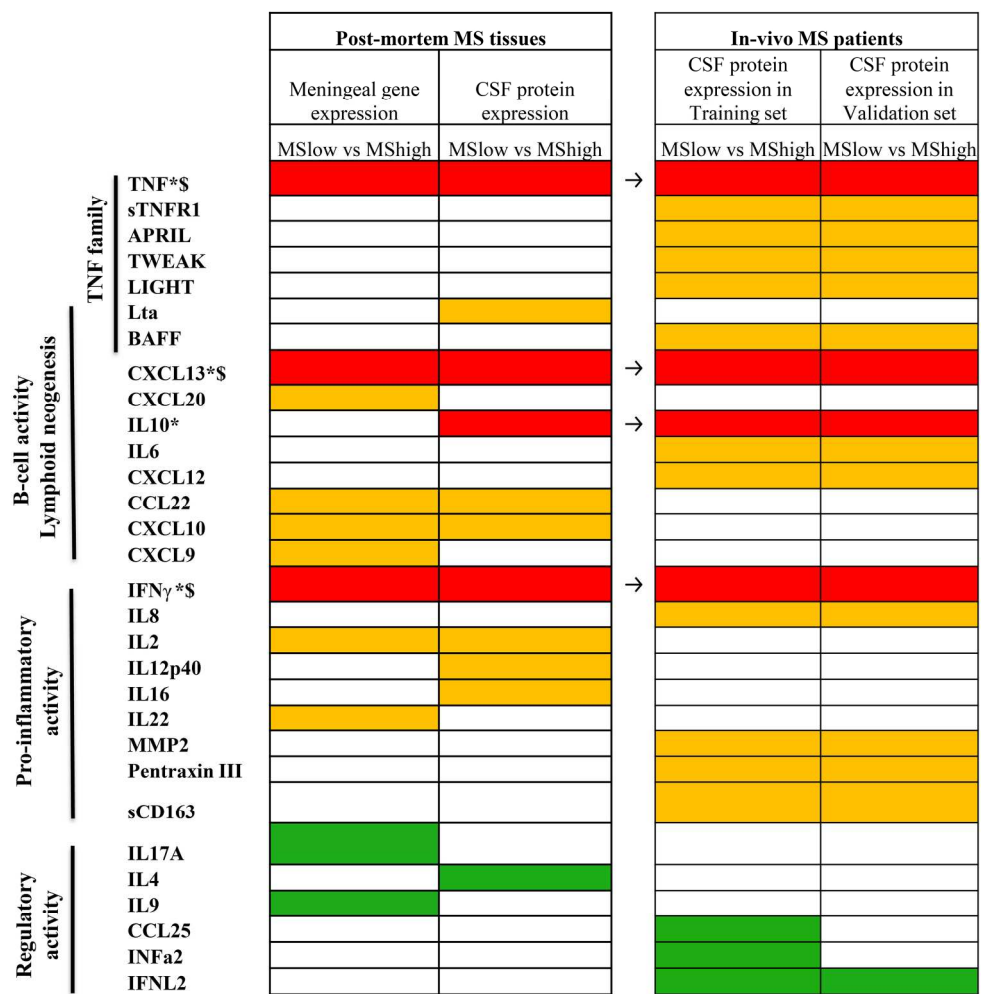


Figure 5

193x196mm (300 x 300 DPI)

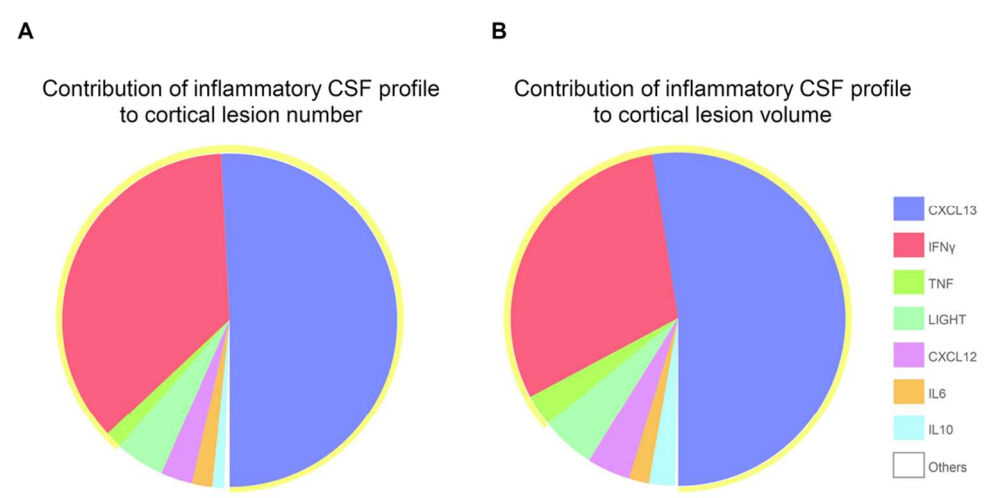


Figure 6

98x51mm (300 x 300 DPI)

Accepted